Kinematics of fibre optics sensory systems for control of a natural gas engine

C O Nwagboso* and **M A Pendlebury**
Transport and Automotive Systems Research Centre, University of Wolverhampton, Telford, Shropshire, UK

Abstract: A fibre optics combustion intensity detection sensor is developed for the purpose of monitoring and controlling natural gas engines. The sensory system, which is based on the detection of the intensity of the combustion event, is mounted on the top of the engine block. Prior to implementation of the detection system, the accurate kinematics of the sensor probe within the combustion chamber needs to be identified while taking account of the geometric complexity of the engine design. This requires the understanding of the kinematics of probe position within the spatial relations of the engine block geometry that is likely to give a good coverage of the combustion processes. This paper therefore presents a new model that was implemented on natural gas engines but could also be used for identifying the appropriate location within the combustion chamber of any modern engine. An application example using the model is presented. The model provides the ability to monitor completely the stages of combustion within the cycle-to-cycle operation of the engine and use the signal thereof for management and control of the engine. Experience gained from the application of the model resulted in the development of the probe deployment rule discussed in this paper.

Keywords: fibre optics, sensors, engine management, ignition control, combustion characteristics

NOTATION

C	cosine
CA	crank angle
EOC	end of combustion
FSD	full-scale deflection
IGN	ignition emission
l	connecting rod length
MBT	maximum brake torque
$\mathbf{P}_{\text{rot}}$	rotation matrix of sensor
$\mathbf{P}_{\text{tran}}$	translation matrix of sensor
r	crank radius
S	sine
SOC	start of combustion
TDC	top dead centre
x_0, y_0	coordinate point at the distal end of sensor
x_i, y_i	coordinate point within the combustion chamber
x_{m}	x plane depth (cylinder bore diameter)
$X_{\text{a}}, Y_{\text{a}}, Z_{\text{a}}$	initial coordinates of sensor
X_A^1, Y_A^1, Z_A^1	new point coordinates of sensor
y_{c}	piston to head clearance height
y_{m}	y plane height (piston to head clearance)
β_0	angle of the distal end
θ	angle of sensor rotation
ϕ	equivalent ratio

The MS was received on 21 July 2000 and was accepted after revision for publication on 9 January 2001.
** Corresponding author: Transport and Automotive Systems Research Centre, University of Wolverhampton, Telford Campus, Shifnal Road, Priorslee, Telford, Shropshire TF2 9NT, UK.*

1 INTRODUCTION

The past decade has experienced increasing interest in the development and application of natural gas as fuel for spark ignition engines. The use of natural gas as engine fuel can be traced back to the 1920s [**1**], but at present, because of the social, health and political pressures to reduce exhaust pollution and to improve air quality, there is the need for continued effort in the research and development of this class of engine. This is the motivation behind the present research in the development of fibre optic sensory systems for combustion intensity and event-based engine management systems.

The typical shape of the optical intensity response that is observed during combustion in an engine using a fibre optic sensor probe is shown in Fig. 1. Where the spark

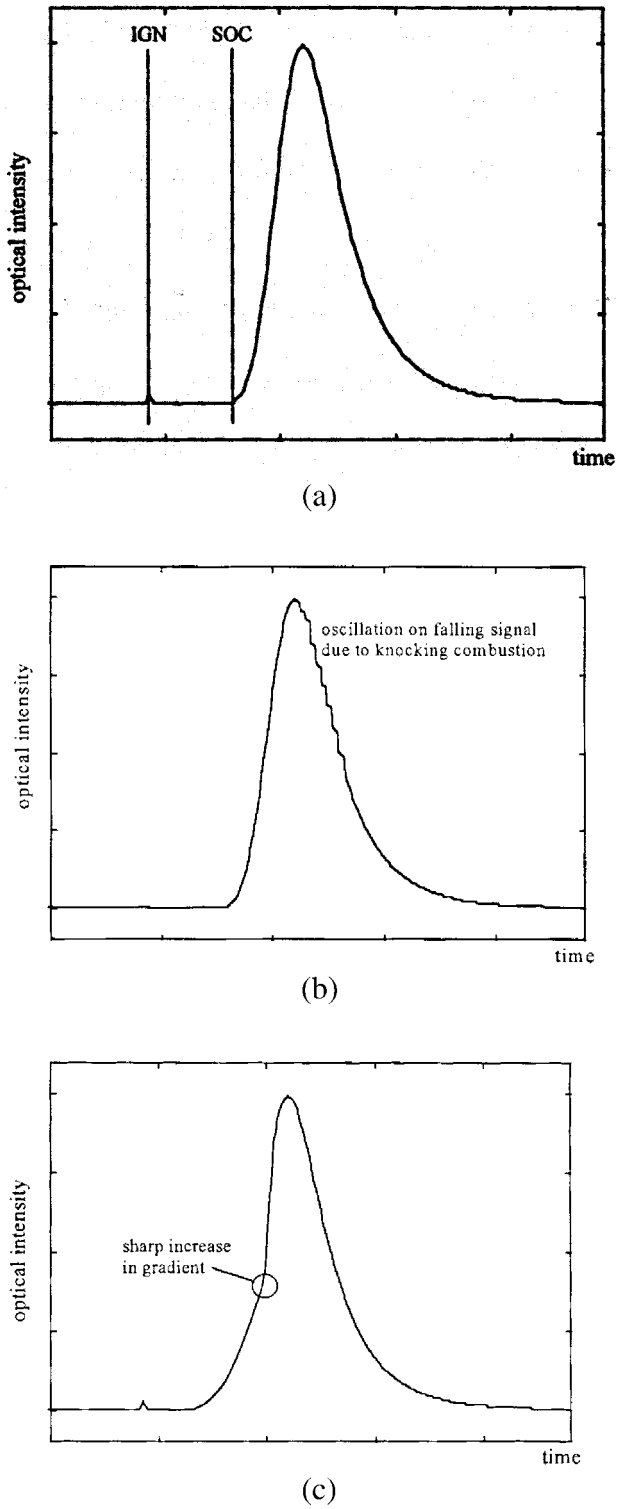

Fig. 1 Typical optical intensity response

plug electrode is within the field of view of the fibre optic sensor, the ignition emission (IGN) will be detected as shown in Fig. 1a. Typically the signal would then begin to rise as the burning mixture enters the field of view of the optical sensor, thus indicating the start of combustion (SOC), and reaching a peak before falling away. Under engine knock conditions, the trailing end of the optical signal can exhibit an oscillatory response shown in Fig. 1b, while under the borderline knock conditions the rising optical signal would exhibit a sharp rise in its rate of increase (Fig. 1c).

Many workers [**2**–**4**] have looked into the use of fibre optic sensors as the basis for combustion event detection. The problem with these sensors is the proper identification of the location of these sensors so that the complete combustion event can be monitored for the purpose of optimum control of the engine. Sasayama [**5**], Takata [**6**] and Day [**7**] have all described different types of sensors for different types of engine, but they have all carried out their research with the problematic 'overheads' of the appropriate location of the sensor probe within the combustion chamber. The present authors [**8**, **9**] and other workers [**10**] have also used the optical fibre sensory technique for control and management of engines; this also occurred with the problematic 'overheads' of the location of the sensor probes. Novel engine control techniques are currently being researched [**11**, **12**] that take advantage of the optical signal offered by a given kinematics of the sensor probe. In this new development, the combination of the optical and pressure sensors can provide the basis for developing an advanced ignition control strategy [**12**, **13**].

Within an appropriate kinematic envelope of a fibre optic sensor, the start of optical emission is widely recognized as an indicator of SOC. This can consequently be used as the basis for developing an engine control algorithm. In one of the experiments carried out by the present authors, the SOC relationship was investigated whereby comparison of the 10 per cent mass fraction burned angle to the 10 per cent level of the normalized optical response was made. Figure 2 shows typical pressure, optical and mass fraction burned response obtained. The comparison of these results indicates the robustness of the optical signal as the basis for engine ignition control.

Therefore, the deciding factor in obtaining and developing the optimum ignition control can depend on the kinematics of the optical sensor with respect to the engine combustion chamber.

2 THE CONSTRAINTS OF SELECTION OF THE MOUNTING SITE OF THE SENSOR PROBE

The free space within the combustion chamber provides the initial constraints in selecting a position for the sensor. Figure 3 indicates the available area on a typical cylinder head face.

In the diagram the potential points at which the probe may enter the cylinder are shown within each specific area numbered. The next stage involves identifying the geometric and environmental restrictions of each of these locations.

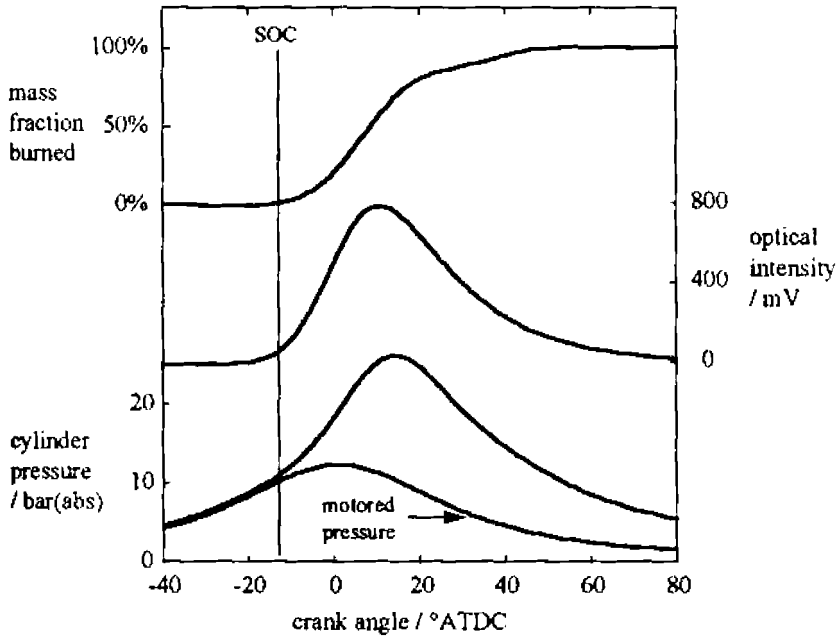

Fig. 2 Optical and pressure signal with mass fractions burned response (ATDC, after top dead centre)

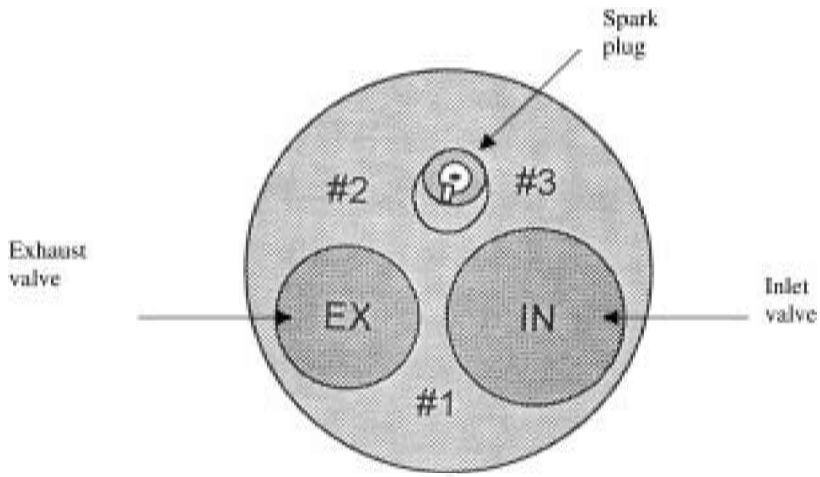

Fig. 3 Potential probe entry sites

1. *Location 1.* This location had several identifiable limitations. The space limitations in this area meant that maximum probe diameter would be limited and the cylinder head strength might be compromised, with potential for creating valve seat problems. In addition, in order to incline the probe to obtain a satisfactory field of view, the probe/sleeve would need to pass through the inlet manifold. Although this can be considered possible, it would increase the complexity and where the sleeve passed through the manifold it would present an airflow disturbance, possibly altering the performance of the respective cylinder.
2. *Location 2.* This sensor or probe position had two favourable features. This part of the head face had the largest available area in which to mount the probe, overcoming the limitation discussed with respect to location 1. In addition, the situation close to the exhaust valve can aid probe self-cleaning owing to the higher average chamber temperature in this area. The proximity close to the exhaust valve can, however, present the potential for increased thermal stressing of the probe as a consequence of this higher temperature.
3. *Location 3.* This offers a slightly reduced face area compared with location 2. The probe position which is close to the inlet valve presented contrasting conditions to location 2. Although both locations 2 and 3 can be considered suitable, this may not be the optimum position, which should give the best coverage of the combustion event.

The best possible entry point of the probe within the chamber having been determined, it is then necessary to

determine the alignment and orientation of its axes. Prior to deciding on the probe orientation, it is important to assess the influence of field of view on the resultant optical response and to explain and resolve any variations in response reported by different workers.

3 ASSESSMENT OF THE EFFECT OF FIELD OF VIEW ON OPTICAL RESPONSE

The most significant variation in the optical profiles observed by previous researchers had been in the phasing of the defining response features. While all this work showed the initial signal rise to correspond to SOC, the principal identifiable difference was in relation to the phasing of peak optical intensity. Although few workers discussed the peak response correlations, of those that did, two clear classifications emerged:

1. Where vertical (e.g. spark plug mounted) probes were employed [**10**], response was found to peak towards end of combustion.
2. With a horizontal probe orientation [**14**, **15**], response mirrored the engine heat release profile, with peak intensity correlating more closely to peak heat release.

These relationships are shown in Fig. 4. This effect was believed to be related to the manner in which the field of view changed over the combustion cycle with respect to the probe orientation.

As shown in Fig. 5, with a vertically mounted design, the field of view of the sensor as a function of chamber volume will increase with a downward piston stroke, emphasizing optical response at later stages of combustion. With the horizontally mounted probe, response is emphasized around top dead centre (TDC). At this point, the field of view gives good coverage of the chamber; however, some reduction in response will occur as the piston descends in the cylinder bore. In this period, around TDC, when bulk combustion occurs, the field of view will be essentially uniform, and thus optical response should correlate more closely with heat release.

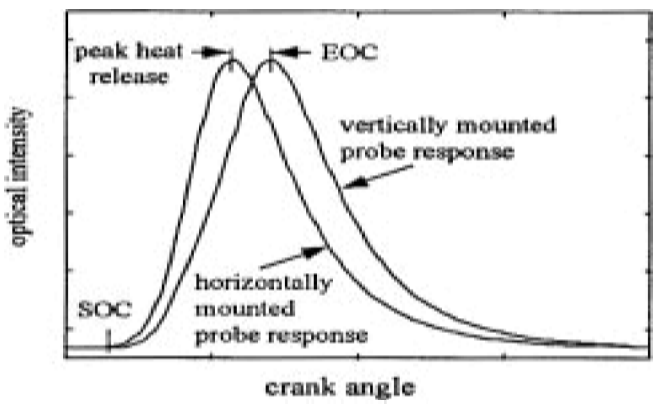

Fig. 4 Response variations for horizontal/vertical probe installations

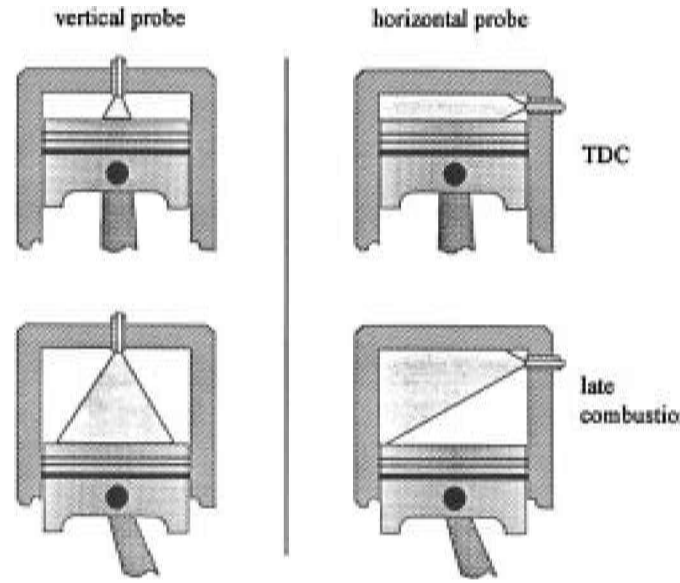

Fig. 5 Variation of field of view with changing crank angle (CA)

4 KINEMATICS OF SENSOR PROBE AS A FUNCTION OF SENSOR GAIN

In order to assess comparatively the influence of the kinematics of the optic fibre probe on the response signal of the sensor, over the engine combustion cycle, it is helpful to develop a kinematic model of the probe. This is a model of the probe position and orientation within the combustion chamber plane. In a global sense, the kinematics is considered on the x–y–z axes of the sensor probe with respect to the chamber, shown in Fig. 6.

Given that a point at the end of the optical sensor probe $[x_A\ y_A\ z_A]$ is known relative to a coordinate system labelled A, a new point $[x_a^1\ y_a^1\ z_a^1]$ can be found that is due to the result of rotating point A of the probe about the z axis through an angle θ. This can be achieved by using a rotation matrix:

$$\begin{bmatrix} \cos\theta & -\sin\theta & 0 \\ \sin\theta & \cos\theta & 0 \\ 0 & 0 & 1 \end{bmatrix} = \text{rotation matrix}$$

The rotation matrix can be multiplied by the original point coordinates $[x_A\ y_A\ z_A]$ to derive the new point:

$$\begin{bmatrix} x_a^1 \\ y_a^1 \\ z_a^1 \end{bmatrix} = \begin{bmatrix} \cos\theta & -\sin\theta & 0 \\ \sin\theta & \cos\theta & 0 \\ 0 & 0 & 1 \end{bmatrix} \begin{bmatrix} x_A \\ y_A \\ z_A \end{bmatrix}$$

The probe can be rotated using a homogeneous coordinate transformation. This can be described by a gen-

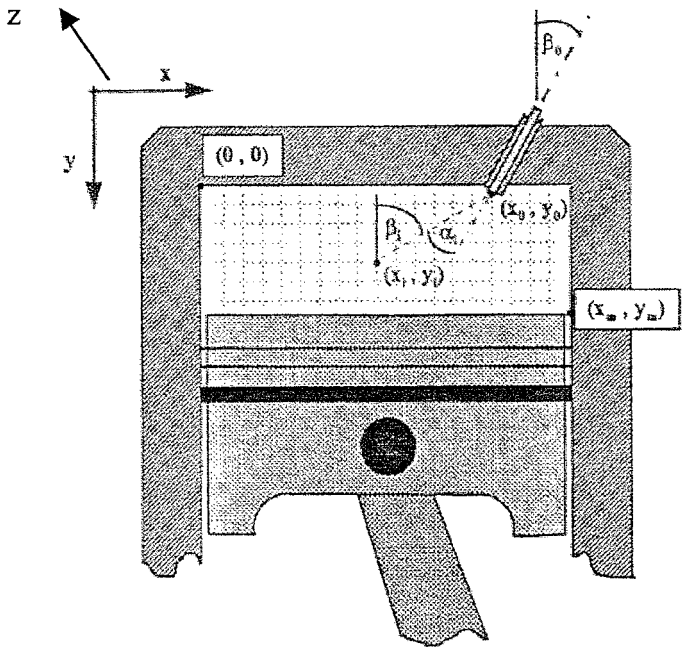

Fig. 6 Optical probe orientation

eralized transformation of a single matrix that combines the effects of translation and rotation of the probe within the boundaries of the combustion chamber. To accomplished this, we can first augment the definition of a wider vector by adding a 1 to it; thus

$$\mathbf{V} = \begin{bmatrix} x \\ y \\ z \\ 1 \end{bmatrix}$$

The rotation matrices can therefore be redefined by making them 4×4 through the addition of a row and a column:

$$\mathbf{P}_{\text{rot}}(x, \theta) = \begin{bmatrix} 1 & 0 & 0 & 0 \\ 0 & \cos\theta & -\sin\theta & 0 \\ 0 & \sin\theta & \cos\theta & 0 \\ 0 & 0 & 0 & 1 \end{bmatrix}$$

$$\mathbf{P}_{\text{rot}}(y, \theta) = \begin{bmatrix} \cos\theta & 0 & \sin\theta & 0 \\ 0 & 1 & 0 & 0 \\ -\sin\theta & 0 & \cos\theta & 0 \\ 0 & 0 & 0 & 1 \end{bmatrix}$$

$$\mathbf{P}_{\text{rot}}(z, \theta) = \begin{bmatrix} \cos\theta & -\sin\theta & 0 & 0 \\ \sin\theta & \cos\theta & 0 & 0 \\ 0 & 0 & 1 & 1 \\ 0 & 0 & 0 & 1 \end{bmatrix}$$

In order to obtain the effect of translation and rotation of the probe, the displacement vector can be placed in the fourth column, thus:

$$\mathbf{P}_{\text{tran}}(a_x, b_y, c_z) = \begin{bmatrix} 1 & 0 & 0 & a_x \\ 0 & 1 & 0 & b_y \\ 0 & 0 & 1 & c_z \\ 0 & 0 & 0 & 1 \end{bmatrix}$$

It is useful to note that matrix multiplication using $\mathbf{P}_{\text{tran}}(a_x, b_y, c_z)$ is equivalent to addition of a 3-vector, where

$$\begin{bmatrix} a_x \\ b_y \\ c_z \end{bmatrix} + \begin{bmatrix} d_x \\ e_y \\ f_z \end{bmatrix} = \begin{bmatrix} a_x + d_x \\ b_y + e_y \\ c_z + f_z \end{bmatrix}$$

and

$$\begin{bmatrix} a_x + d_x \\ b_y + e_y \\ c_z + f_z \\ 1 \end{bmatrix} = \begin{bmatrix} 1 & 0 & 0 & a_x \\ 0 & 1 & 0 & b_y \\ 0 & 0 & 1 & c_z \\ 0 & 0 & 0 & 1 \end{bmatrix} \begin{bmatrix} d_x \\ e_y \\ f_z \\ 1 \end{bmatrix}$$

The combination of probe rotations and translations can also be accomplished by a matrix multiplication. For example, the probe can be imagined to be rotated to 90° about the z axis, followed by a rotation of 90° about the x axis and subsequently completed by the probe translation of $[d_x\ e_y\ f_z]^{\text{T}}$. The effect of these rotations and translations on an initial point on the probe, $[a_x\ b_y\ c_z]^{\text{T}}$, can be found.

The resultant effect on the probe will be

$$\mathbf{P}_{\text{tran}}(d_x, e_y, f_z)\mathbf{P}_{\text{rot}}(x, 90^\circ)\mathbf{P}_{\text{rot}}(z, 90^\circ) \begin{bmatrix} d_x \\ b_y \\ c_z \\ 1 \end{bmatrix}$$

$$= \begin{bmatrix} 1 & 0 & 0 & d_x \\ 0 & 1 & 0 & e_y \\ 0 & 0 & 1 & f_z \\ 0 & 0 & 0 & 1 \end{bmatrix} \begin{bmatrix} 1 & 0 & 0 & 0 \\ 0 & 0 & -1 & 0 \\ 0 & 1 & 0 & 0 \\ 0 & 0 & 0 & 1 \end{bmatrix}$$

$$\times \begin{bmatrix} 0 & -1 & 0 & 0 \\ 1 & 0 & 0 & 0 \\ 0 & 0 & 1 & 0 \\ 0 & 0 & 0 & 1 \end{bmatrix} \begin{bmatrix} a_x \\ b_y \\ c_z \\ 1 \end{bmatrix}$$

$$= \begin{bmatrix} 1 & 0 & 0 & d_x \\ 0 & 0 & -1 & e_y \\ 0 & 1 & 0 & f_z \\ 0 & 0 & 0 & 1 \end{bmatrix} \begin{bmatrix} -b_y \\ a_x \\ c_z \\ 1 \end{bmatrix}$$

$$= \begin{bmatrix} -b_y + d_x \\ -c_z + e_y \\ d_x + f_z \\ 1 \end{bmatrix}$$

The above matrix multiplication is associative: the first two matrices are combined into a single matrix by multiplying them together. This can be done by a single matrix, which is a homogeneous transformation.

Matrix multiplication is not commutative, and hence

$$\mathbf{P}_{\text{rot}}(x, \theta)\mathbf{P}_{\text{rot}}(y, \phi) \neq \mathbf{P}_{\text{rot}}(y, \phi)\mathbf{P}_{\text{rot}}(x, \theta)$$

A general form of the probe transformation matrix can be developed. If the probe rotates ϕ_z about z, and further rotates ϕ_y about y, and finally rotates ϕ_x about x, the resultant rotation of the probe can be defined as combination rotation such that

$$\mathbf{P}_{\text{rot}}(\phi_z, \phi_y, \phi_x) = \mathbf{P}_{\text{rot}}(z, \phi_z)\mathbf{P}_{\text{rot}}(y, \phi_y)\mathbf{P}_{\text{rot}}(x, \phi_x)$$

If the above equation is expanded using cosines and sines as appropriate, the following is derived:

$$\mathbf{P}_{\text{rot}}(\phi_z, \phi_y, \phi_x) = \begin{bmatrix} C\phi_z C\phi_y & C\phi_z S\phi_y S\phi_x - S\phi_z C\phi_x & C\phi_z S\phi_y C\phi_x + S\phi_z S\phi_x & 0 \\ S\phi_z C\phi_y & S\phi_z S\phi_y S\phi_x - C\phi_z C\phi_x & S\phi_z S\phi_y C\phi_x + C\phi_z S\phi_x & 0 \\ -S\phi_y & C\phi_y S\phi_x & C\phi_y C\phi_x & 0 \\ 0 & 0 & 0 & 1 \end{bmatrix}$$

where S denotes sine and C cosine. In this combined matrix, the translation of the probe can be included by replacing the zeros in the fourth column with a_x, b_y, c_z and therefore a complete transformation matrix, including three rotations and three translations is obtained.

This transformation of the probe assumes that the angle of the probe end distal surface is constant. If the change in the end distal surface inside the combustion chamber is varied, then the transformation should take account of that change.

5 EXPERIMENTAL RESULTS

5.1 Test engine

The engine selected for the test programme was a Ford Kent 1600 cm^3 four-cylinder four-stroke cross-flow unit. The power unit is an overhead valve design with a compression ratio of 9 : 1. An industrial fan-cooled radiator unit was fitted in front of the engine. The engine-driven fan provided cooling airflow over the engine block and through the radiator unit.

5.2 High-speed data acquisition system

As shown in Fig. 7, an Amplicon PC226 16-channel high-speed data acquisition card was used to enable the capture of combustion-related parameters. This unit was selected as it offered considerable scope to configure the unit flexibly for data acquisition. The data acquisition unit operated independently of another moderate speed data acquisition system used on the test rig. It featured 12-bit sampling, giving signal resolution of 0.024 per cent of full-scale deflection (FSD). An important feature of the unit was that it allowed external triggering of data acquisition. This allowed sampling to be synchronized to engine CA rather than time and led to easier analysis and comparison of the data. A 1° CA trigger signal was derived from the Microsync $\frac{1}{4}$° synchronization signal and used for this purpose.

A second important feature was the wide span of configurable gain settings. Each channel could be configured independently over 16 gains from 10 V FSD to 1.25 mV FSD, unipolar or bipolar. This offered great flexibility in ensuring that the most suitable gain span could be selected to match the anticipated input signal span. The maximum sampling frequency of the unit was 1 MHz. The maximum sample frequency used in this work was limited to

$$\frac{3000 \text{ r/min}}{60} (\text{max tested engine speed/Hz}) \times 360$$
$$= 18 \text{ kHz}$$

The PC226 was software controlled by its host PC.

In the present study, the model developed previously is reduced to a two-dimensional model. This was considered adequate to allow the indication of the general trends by which the signal gain changes over the combustion cycle. The model generates an overall gain factor which indicates how effectively the field of view covers the combustion space for a given probe position and orientation. This gain factor is expressed in terms of the average response of the sensor over the complete combustion chamber plane. The model simplifies the actual chamber by only considering the plane in which the sensor is mounted, but this will nevertheless enable comparative assessment of different probe orientations. As shown in Fig. 8, the sensor distal end position and orientation are constrained to three degrees of freedom, these being the x, y position within the chamber and the probe inclination angle. Only a symmetrical probe end shape can be catered for by this simple model.

If the probe distal end is situated at a position x_0, y_0 and at an angle β_0, the deviation angle from the probe axis of any point within the chamber can be deduced. For a point within the chamber (x_i, y_i), the angle β_i can be determined from a simplified equation:

$$\beta_i = \tan^{-1}\left(\frac{x_0 - x_i}{y_i - y_0}\right)$$

and hence the deviation from the probe axis, α_i, is given

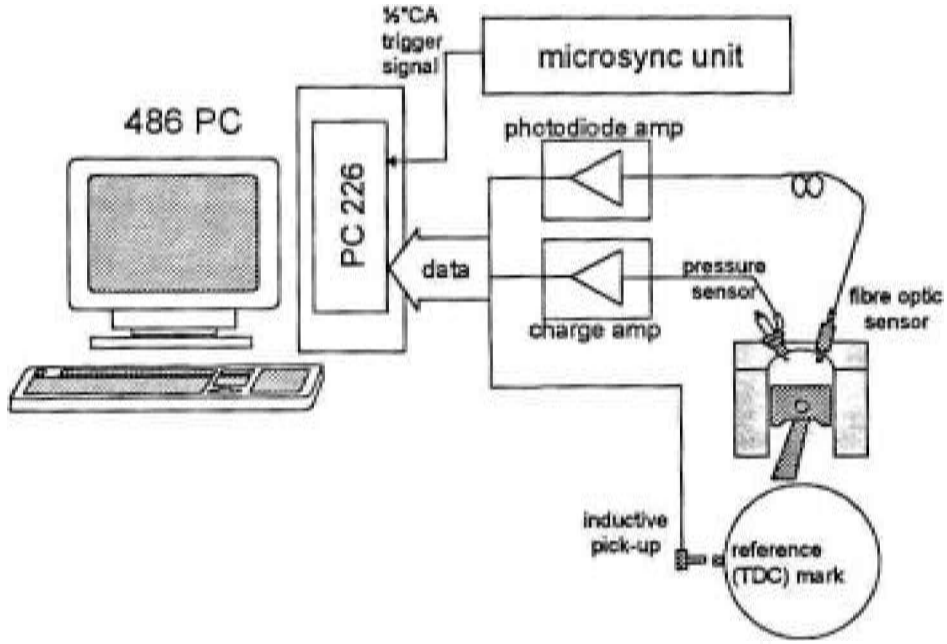

Fig. 7 Schematic of the combustion data acquisition system

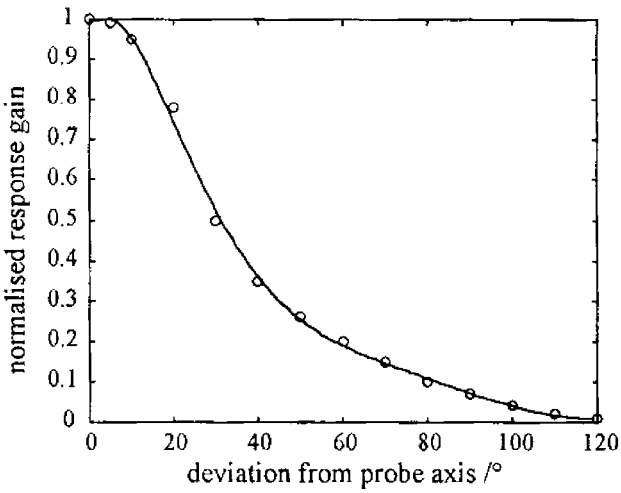

Fig. 8 Modelling probe response

by

$$\alpha_i = |\beta_i - \beta_0|$$

The sensitivity of the probe to luminous emission from any spatial point will be a function of the deviation angle from the probe axis of that point. This response has been experimentally determined from the hemispherical end shape used in this work [**9**] and is shown in Fig. 9.

Hence for any position (x_i, y_i) within the chamber, the response gain Ω will be given by

$$\Omega = f_0(\alpha_i)$$

where f_0 represents the response profile. Consider a flat cylinder head and flat-topped piston, with a plane section of width x_m. If the engine has a clearance height from the cylinder head of y_c, then, for any CA θ, the depth

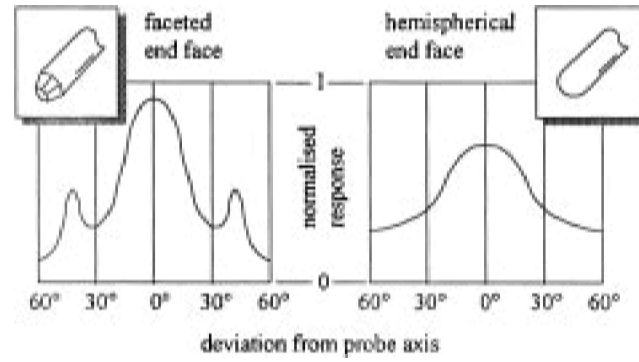

Fig. 9 Angular response of sensor

of the plane, y_m, will be given by

$$y_m = y_c + r\left[1 + \frac{l}{r} - \cos\theta - \sqrt{\left(\frac{l}{r}\right)^2 - \sin^2\theta}\right]$$

where

y_c = piston to head clearance height
r = crank radius (stroke/2)
l = connecting rod length

The average gain at any CA, θ, will then be given by

$$\Omega_\theta = \frac{\sum_{0,0}^{x_m, y_m} f_0[\alpha(x_i, y_i)]}{x_m y_m}$$

where

$x_m = x$ plane depth (cylinder bore diameter)
$y_m = y$ plane height (piston to head clearance)
$x_i = x$ coordinate position
$y_i = y$ coordinate position

Dividing by the area of the chamber plane gives the average gain of the sensor response over the entire chamber plane.

An algorithm was constructed based on this theoretical analysis to allow the response for various probe orientations and positions to be determined. This was coded as a Matlab '.m' file.

Typical test conditions that were used in the experimental work covered the major operating speed range of the engine. The test conditions are summarized as a test point matrix in Table 1. Using these test parameters, the optical signals were sampled at a resolution of 1° CA/sample, with 19–20 consecutive combustion cycles typically captured.

The primary objective of the test was to identify aspects of the optical response which could be applied to engine control. However, there were other secondary goals associated with the testing. These included a means of interpreting the optical response in terms of combustion-defining parameters, such as mass fraction burned, cylinder pressure and heat release. For a given kinematics, this facilitated comparison of test results and the understanding of the optical emission in terms of combustion dynamics. These comparisons have been made by the present authors in previous research [**9**].

Table 1 Test point matrix

Test parameter	Range
Speed	1500–3000 r/min; 500 r/min increments
Load	0.42, 0.22, 0.01 bar (manifold depression)
Timing	30° CA span centred at maximum brake torque (MBT) timing; 5 increments

5.3 Engine control scheme

As has been cited in a previous section of this paper, several methods of control schemes can be used for controlling the engine, based on the optical signal obtained from the sensor. In developing the control scheme for the work reported in this paper, two ignition control schemes were considered. The first was ignition control based on the peak optical intensity position and the second was ignition timing control based on peak rate of increase of the optical signal. In each of the cases, the kinematics of the optical sensor influenced the integrity of the optical signal. However, both control schemes are essentially similar in principle. The architecture of the second control scheme is shown in Fig. 10. With this scheme, the optical signal peak was first measured and used to switch the data acquisition unit to a lower gain if a preset threshold is exceeded or a higher gain if a lower threshold level is not attained. This is necessary because of the possible variation of peak optical intensity with varying load and also with varying ignition timing.

The signal rate was measured by differencing consecu-

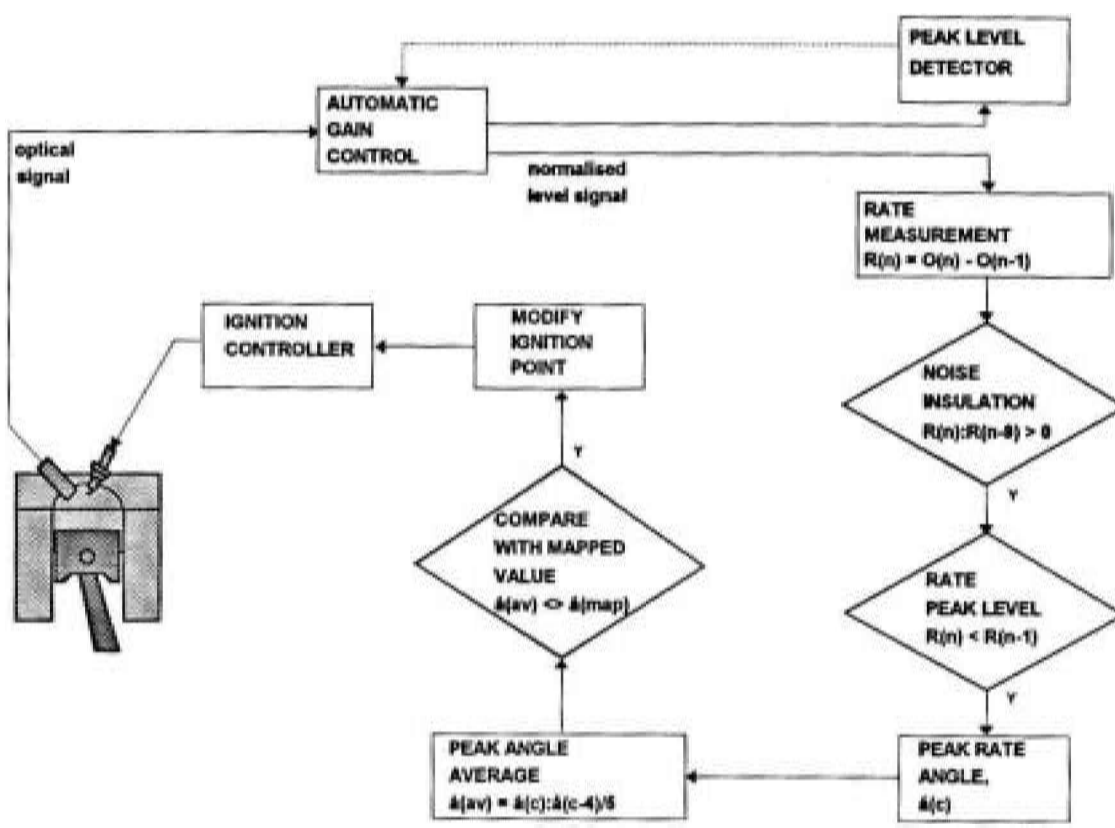

Fig. 10 Ignition controller system processing architecture

tive sample levels, and the rate signals were then checked to ensure a rising trend over a typical 5° CA period. This helped to insulate the system effectively from short duration noise spikes. The system detected when the rate signal reaches a maximum, and the CA of this maximum is stored. The control algorithm averages these angles over 5–10 cycles in order to limit the effect of cyclic variability on the control system. Where this averaged signal deviates from the desired map referenced value, a correction is applied to the ignition point. This was, in this case, again limited to $\pm 1°$ per 5 cycles to provide smooth transitional control. It is important to note that the scheme described here allows a simple control algorithm with a low computer processing overhead to be used for the engine—this is in contrast to other methods such as those using knock sensors.

6 THEORETICAL MODEL RESULTS

Using the model, the response profiles for a range of probe orientations covering those most widely employed in previous work were evaluated. These orientations are shown in Fig. 11 and summarized in Table 2.

The test engine dimensions were used in the model, with x_m represented by bore diameter. Since the engine was of bowl-in-piston design, y_c was taken as the mean height between bowl clearance and top land clearance at TDC. These parameters are summarized in Table 3.

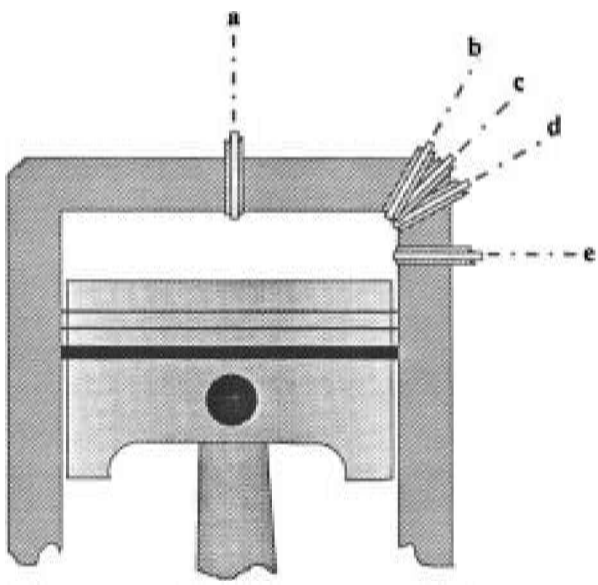

Fig. 11 Modelled probe locations

Table 2 Location parameters

Location	θ_0	x_0	y_0	Description
a	0°	$x_m/2$	0	Vertical central location
b	30°	x_m	0	Angled corner location
c	45°	x_m	0	Angled corner location
d	60°	x_m	0	Angled corner location
e	90°	x_m	$y_c/2$	Horizontal location

The resultant response gains for each position are shown in Fig. 12. In general it can be seen that the closer the probe inclination is to the vertical plane, the greater will be the average gain as the piston descends. Conversely, for a horizontally mounted probe, average gain falls away as the probe descends.

A further factor, which must be considered when interpreting these results, is how the developing flame front will modify sensor response. Because the location of this flame front will be well defined during early combustion and around TDC, then, provided that the probe is aligned to view this early combustion, the actual gain of the sensor will be emphasized close to TDC. The magnitude by which this will modify the gain is difficult to quantify since this effect would ultimately be based on a prediction of how the flame front will develop spatially. It does, however, allow general qualitative assessment of the overall optical gain.

7 INTERPRETATION OF PUBLISHED RESULTS USING THE THEORETICAL MODEL

Although past workers have employed engines with widely varying chamber shape, the general findings of this basic model help to resolve the difference in peak optical response found by some of these workers. The work of Nutton and Pinnock [**10**] found that response

Table 3 Ford test engine data

Bore	80.98 mm
Connecting rod length	125.17 mm
Crank radius	38.81 mm
Bowl–head clearance at TDC	17 mm
Top land–head clearance at TDC	3 mm
Mean clearance at TDC	11.1 mm

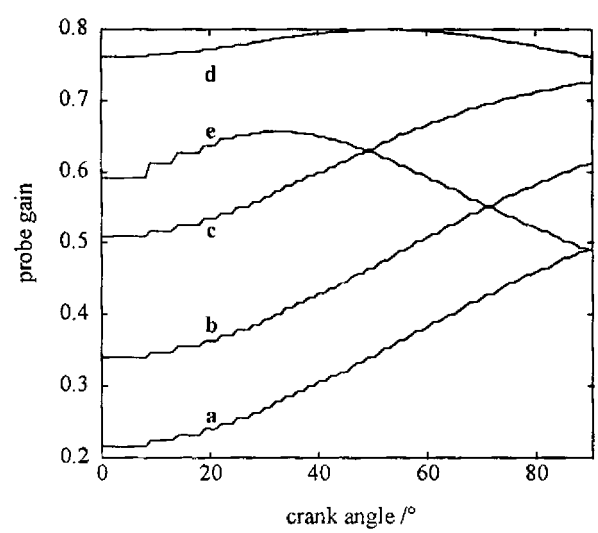

Fig. 12 Average response for probe locations examined

peaked in late combustion when using a vertical spark plug mounted probe. This will be due to the increase in average gain as the piston descends, emphasizing the output during later combustion, as was shown by response a of Fig. 12. Other workers [**14**, **15**] found a correlation between optical response and heat release using a horizontally aligned probe. From the model response e it can be seen that this alignment gives a more uniform gain, and thus the optical profile would be expected to correlate closely with heat release rate [**9**].

8 GENERAL DEPLOYMENT RULES FOR SELECTING SENSOR ORIENTATION

For the flat cylinder head chamber used in this work, with a hemispherically ended sensor, the model results have allowed some general rules to be specified that can enable the optical response to be predicted for a given deployment scenario. These are as follows:

1. Vertically mounted probes will give a response which peaks during the late stages of combustion.
2. Horizontally mounted probes will have a response emphasized around TDC, with the average system gain falling during late combustion.
3. If the probe is aligned to view the early development of combustion (around the spark plug), response will be emphasized during early stages of combustion, giving an average gain level above that predicted by the model during this time.
4. Provided that rule 3 is observed, it is proposed that the most uniform response over the whole combustion cycle will be obtained by aligning the probe at an angle of 45°.
5. If this is not possible because of the presence of casting obstructions or external engine features, it is suggested that a probe orientation angle of between 30° and 60° will yield acceptable uniformity of gain.

On the basis of this assessment, the principal objective would then be to orient the probe to achieve best uniformity of gain, and also to maximize the field of view, given the geometric constraints which existed. As shown in Fig. 13, maximizing sensor field of view to cover a large an acceptance angle as possible offers the scope to customize the response. For example, should detection of emission from a specific area of the chamber be required, then the end face of the probe could be modified to emphasize response in that region.

Figure 14 shows the final selected position and orientation of the probe within the cylinder head of a natural gas engine system developed by the present authors. The 40° inclination angle was close to the optimum 45° inclination, given the physical constraints on installation. In this experimental test bed, the 72° angle was selected to ensure that the probe axis was as closely aligned to the spark plug axis as possible. This is to ensure the emphasis

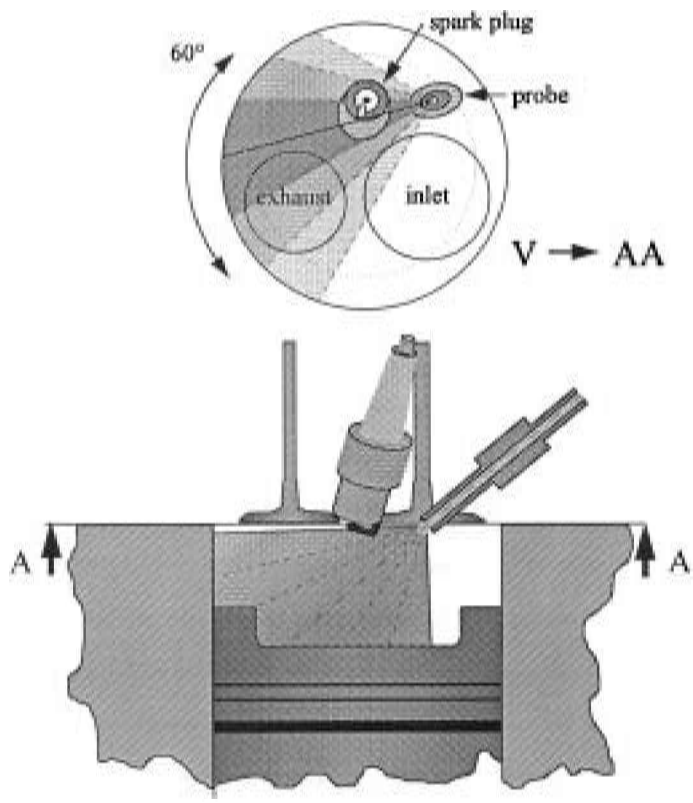

Fig. 13 Optical probe field of view

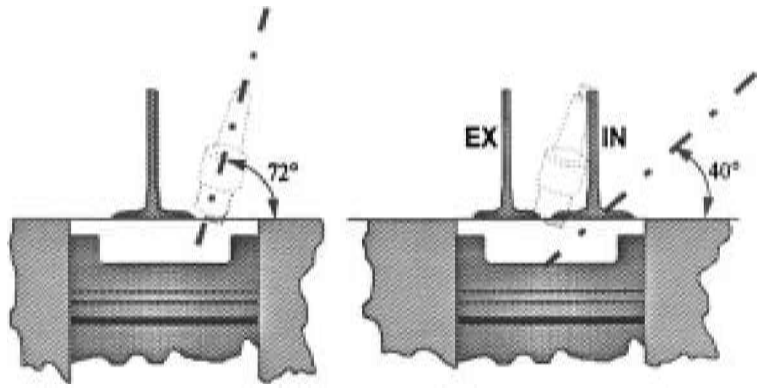

Fig. 14 Probe orientation

of early flame development in the cylinder. In the experimental test rig developed, this position was felt to give the widest field of view while allowing ease of connection to the fibre optic cable outside the cylinder head.

Furthermore, at 70° orientation angle of the probe, the correlation between the peak optical intensity angle and engine torque was investigated. A sample of the results is shown in Fig. 15. It can be seen from the results that peak torque of the engine occurred at peak optical intensity that corresponds to a specific CA. For the test engine used in the experiment, this angle was found to be at 12°–13° ATDC. This relationship was confirmed to be independent of speed and load. The results obtained also cover equivalence ratio from $\phi = 0.75$ to $\phi = 0.86$, which suggests that this relationship is also independent of air–fuel ratio. This indicated that peak optical intensity angle could be an ideal parameter on which to base an ignition timing control scheme capable of enabling the determination of MBT timing with no additional engine sensors being required.

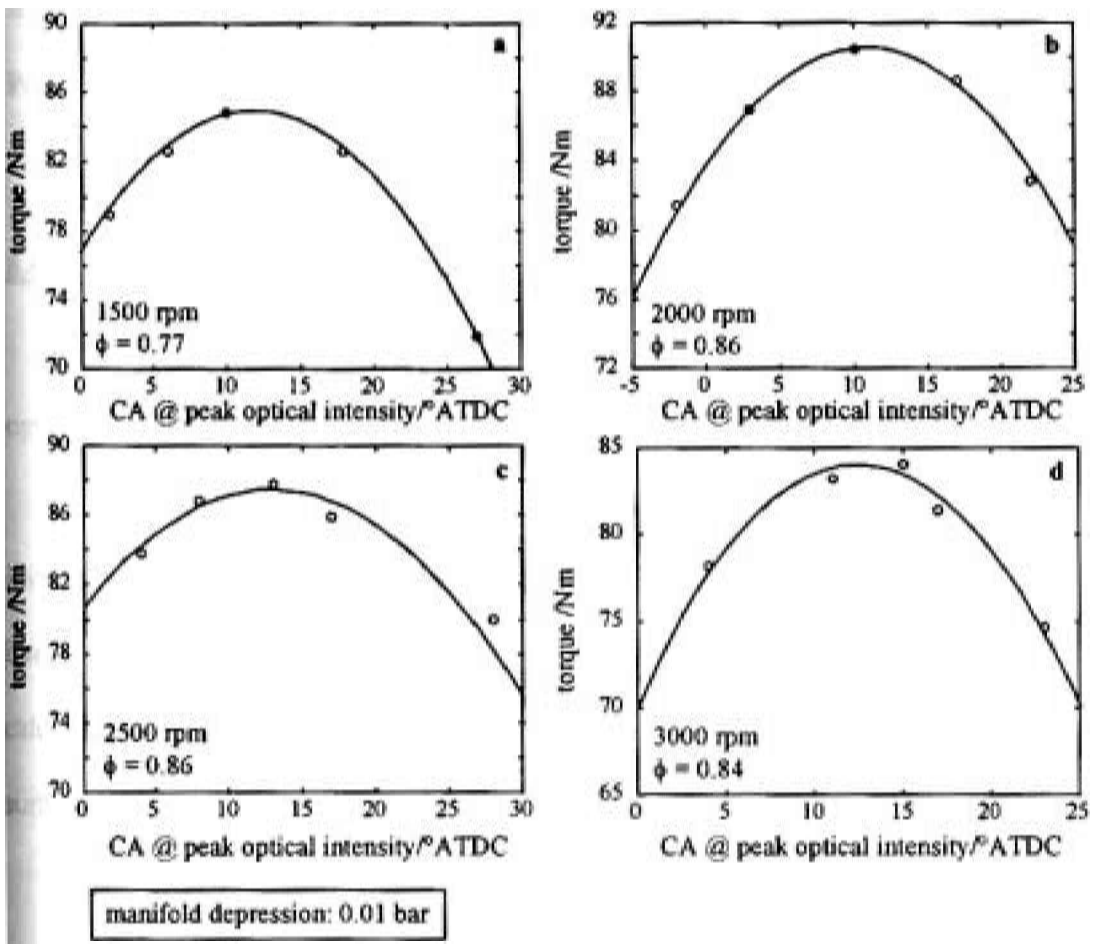

Fig. 15 Relationship between CA at peak optical intensity and engine torque at engine mid-load

9 CONCLUSIONS

A model has been developed for solving the problem of fibre optics sensor probe location for a better and wider coverage of the combustion events in an engine combustion chamber. The model only considers the kinematics of the probe based on a practical probe orientation. An example shows that the model can be used for assessing the signal gain, which relates to the combustion and optical intensity of the sensor. On the basis of the knowledge developed as a consequence of this model, a general rule for selection of the probe orientation has been presented. Further work is currently in progress for developing a more complex algorithm, which will give a three-dimensional mapping of the combustion event for the purpose of engine control and management. An alternative use of the optical signal obtained under this complex mapping condition would be to exploit the optical signal for controlling combustion processes.

The probe kinematics developed in this present research has been based on the assumption that the measured performance of one cylinder provides an accurate predictor of the general performance of the engine. However, each cylinder of the multicylinder engine would have a differing intake charge composition owing to variation in manifold tract geometry. It will also operate at different temperatures from cylinder to cylinder. These differences will inevitably lead to combustion variation from cylinder to cylinder which will, to some degree, result in different optimum ignition angles. In order to measure the magnitude of the variation, it is recommended that users of the techniques presented in this paper carry out further development trials, on multiprobes and multicylinder engines. These trials may initially take the form of measuring cylinder pressure and optical intensity for each cylinder at reference operating conditions. Mass fraction burned analysis of these data would then indicate the extent of any variation in the 50 per cent burn angle from cylinder to cylinder. More significantly, it will determine whether any variation remained consistent with changing operating points.

REFERENCES

1 **Zwemmer, A.** Compact high pressure natural gas compression for CNG refuelling system. *Sulzer Tech. Rev.*, 1987, **2**, 3–7.

2 **Pinnock, R. A.**, *et al.* Combustion sensing using optical fibres. In IEE Sixth International Conference on *Automotive Electronics*, 1987.

3 **Balardini, P.** Ignition measurement in a direct injection diesel engine. In Proceedings of IMechE International Conference on *Combustion in Engineering*, 1983, Vol. 2, paper C86/83, pp. 1–8 (Institution of Mechanical Engineers, London).

4 **Moser, W.** Light sensing in an Otto-combustion engine. In Proceedings of Twentieth FISITA Congress, 1984, paper 845002.

5 **Sasayama, T.** Recent development of optical fibre sensors for automotive use. *Fibre Integrated Optics*, 1987, **7**, 255–271.

6 **Takata, M.** Development of optical combustion timing sensor for a diesel engine. In Proceedings of Sixteenth ISATA Conference, Italy, 1987.

7 **Day, E.** Start of combustion sensor. SAE paper 890484, 1989.

8 **Pendlebury, M. A.** and **Nwagboso, C. O.** Control of ignition on SI engines using an optical sensor. In Proceedings of International Conference on *Road Vehicle Automation*, UK, 1995.

9 **Pendlebury, M. A.** and **Nwagboso, C. O.** An optical sensor for determination of combustion parameters in a natural gas fuelled spark ignition engine. SAE paper 960856, 1996.

10 **Nutton, D.** and **Pinnock, R. A.** Closed loop ignition and fuelling control using optical combustion sensor. SAE paper 900486, 1990.

11 **Nwagboso, C. O., Wang, W., Zouh, E.** and **Lee, C.** Design consideration for fuzzy logic control of natural gas engines. In IEEE Intelligent Vehicle Symposium, Germany, 1998.

12 **Wang, W., Chirwa, C., Holmes, K., Zhou, E.** and **Nwagboso, C. O.** Fuzzy ignition timing control for a spark ignition engine. *Proc. Instn Mech. Engrs, Part D, Journal of Automobile Engineering*, 2000, **214**(D3), 297–306.

13 **Wang, W., Nwagboso, C. O., Zhou, E.** and **Lee, C.** Intelligent ignition control of using pressure sensors with fuzzy logic in natural gas engines. In Proceedings of IEEE International Conference on *Intelligent Vehicles (IV98)*, Germany, 1998.

14 **Beshai, S.** Chemiluminescence—a diagnostic technique for internal combustion engines. In *Application of Fluid Mechanics*, ASME Fluids Engineering Division FED, Vol. 100, 1990, pp. 115–118.

15 **Nagase, K.** and **Funatsu, K.** A study of NO_x generation mechanism in diesel exhaust gas. SAE paper 901615,1990.